Supplementary Information

Porous metal microsphere M@C-rGO (Metal = Mn, Fe, Co, Ni, Cu) aerogels with high low-frequency microwave absorption, strong thermal insulation and excellent anticorrosion performance

Junfeng Qiu[a], Xin Liu[a], Chunyi Peng[a], Sihan Wang[a], Rongchen Wang[a], Wei Wang[a,b*]

[a] Department of Physics and Electronics, School of Mathematics and Physics, Beijing University of Chemical Technology, Beijing 100029, China

[b] Beijing Key Laboratory of Environmentally Harmful Chemical Analysis, Beijing University of Chemical Technology, Beijing 100029, China

[*] Corresponding authors. E-mail: wangwei@mail.buct.edu.cn

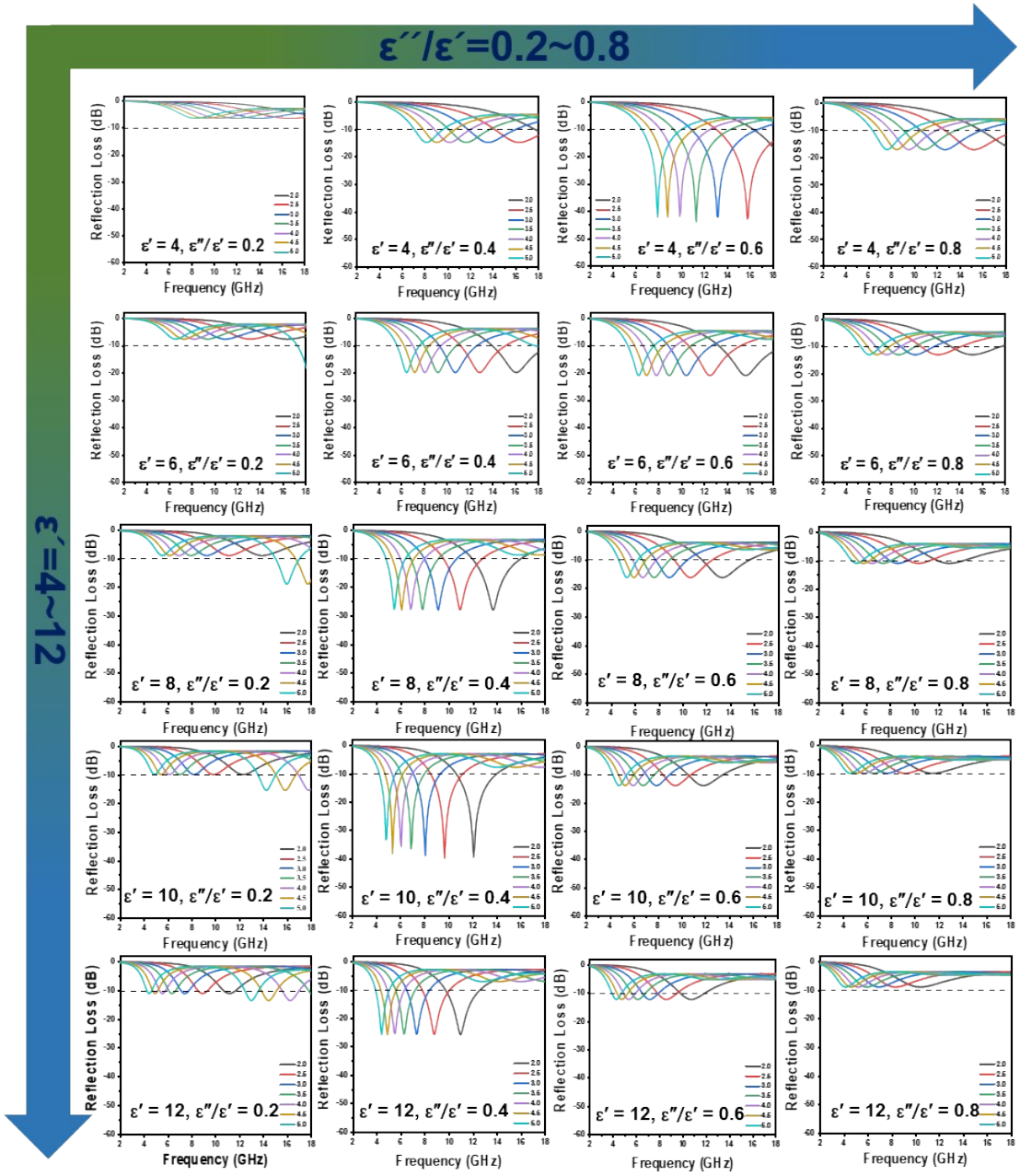

Figure S1. Numerical simulation of complex dielectric constant ($\mu' = 1$, $\mu'' = 0$).

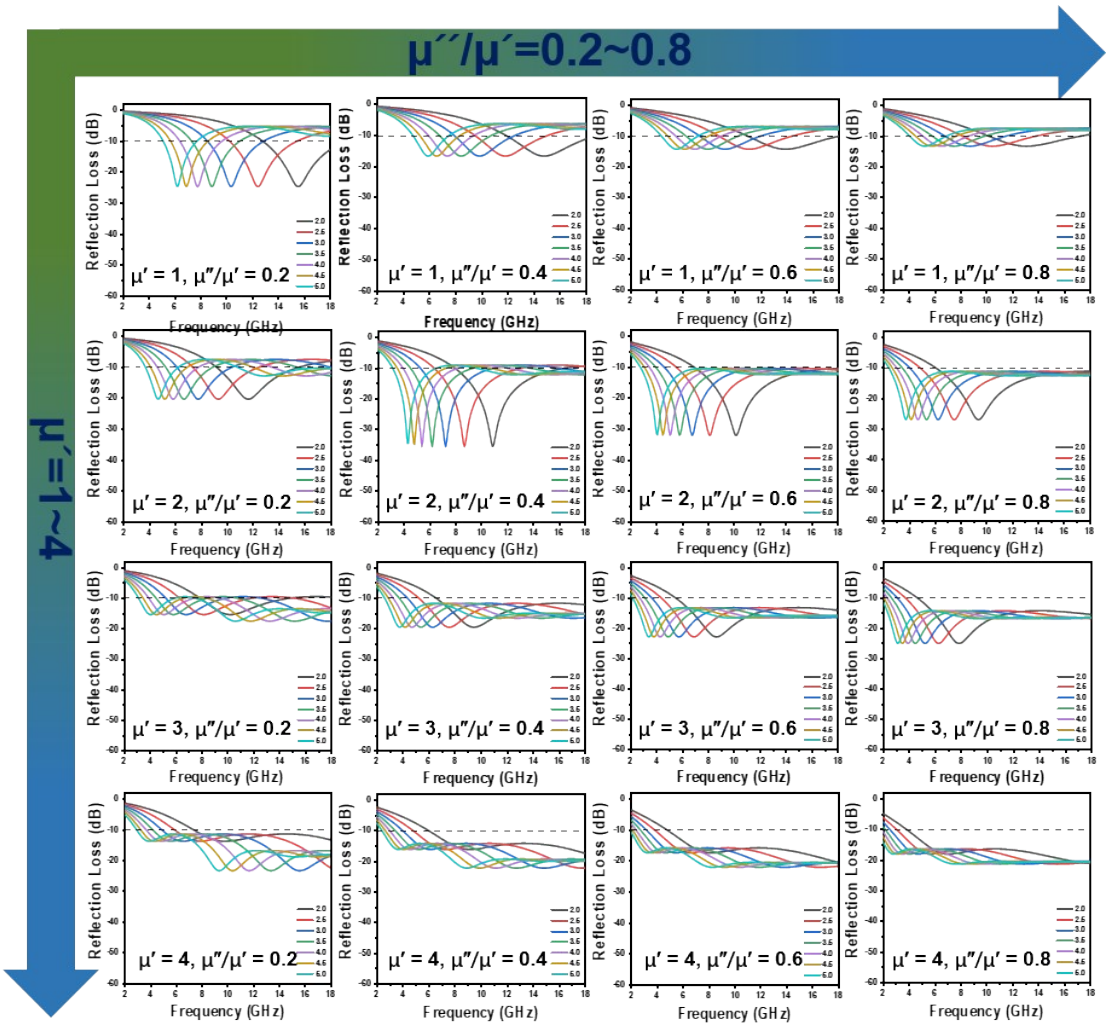

Figure S2. Numerical simulation of complex permeability ($\varepsilon' = 6$, $\varepsilon'' = 2.4$).

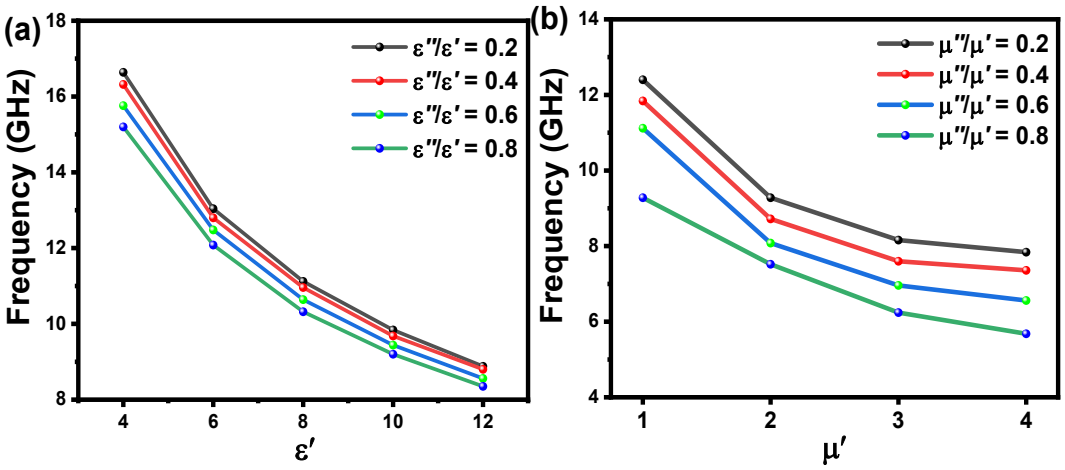

Figure S3. The RL_{min}@Frequency for numerical simulations at a thickness of 2.5 mm.

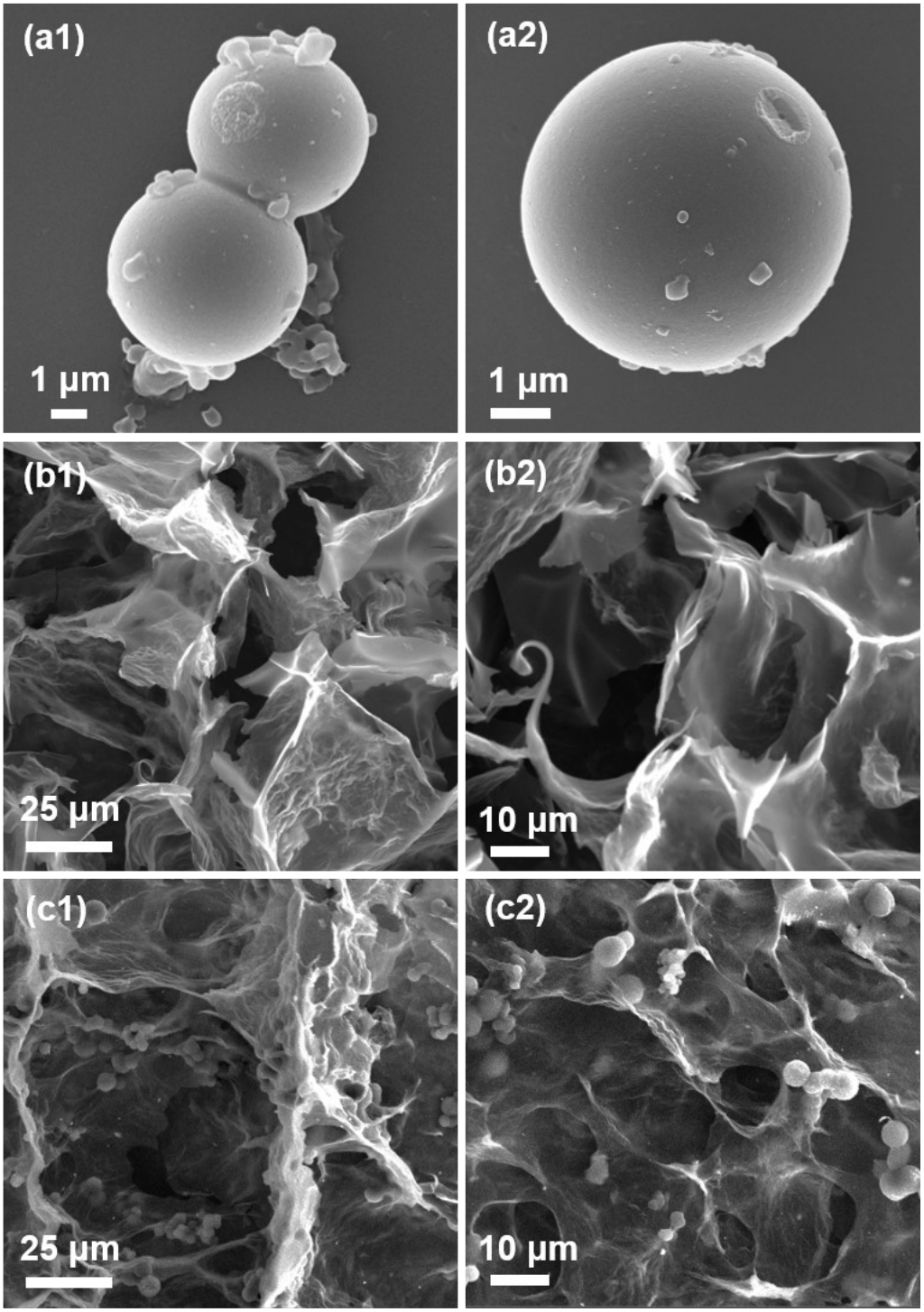

Figure S4. The SEM images of the sample a) Cu-p, b) C-rGO, c) Cu@C-rGO.

Figure S5. The actual images of the as-synthesized sample Cu@C-rGO.

Figure S6. The actual images of the as-synthesized samples M@C-rGO.

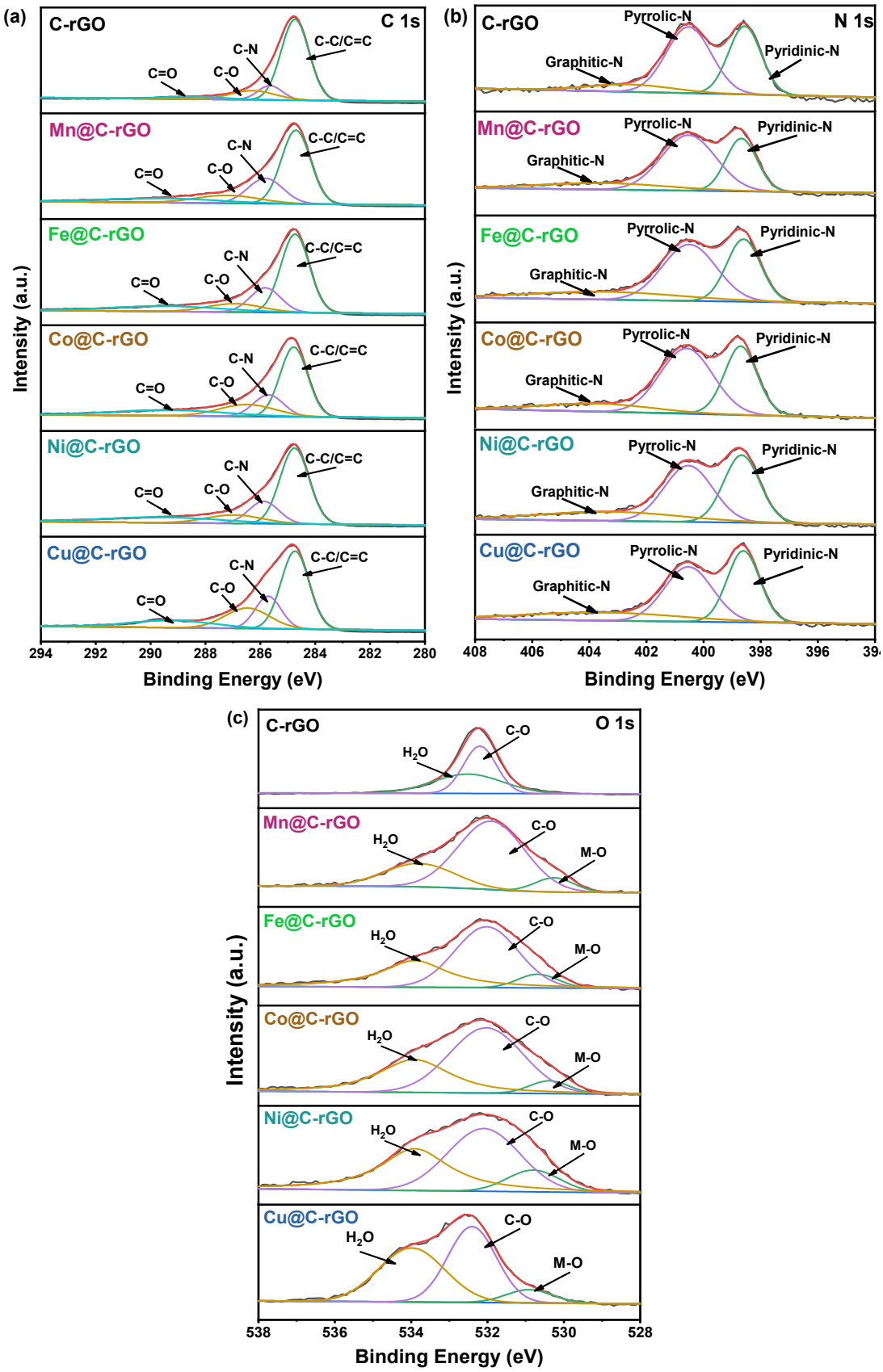

Figure S7. The high-resolution XPS spectra of a) C 1s, b) N 1s and c) O 1s.

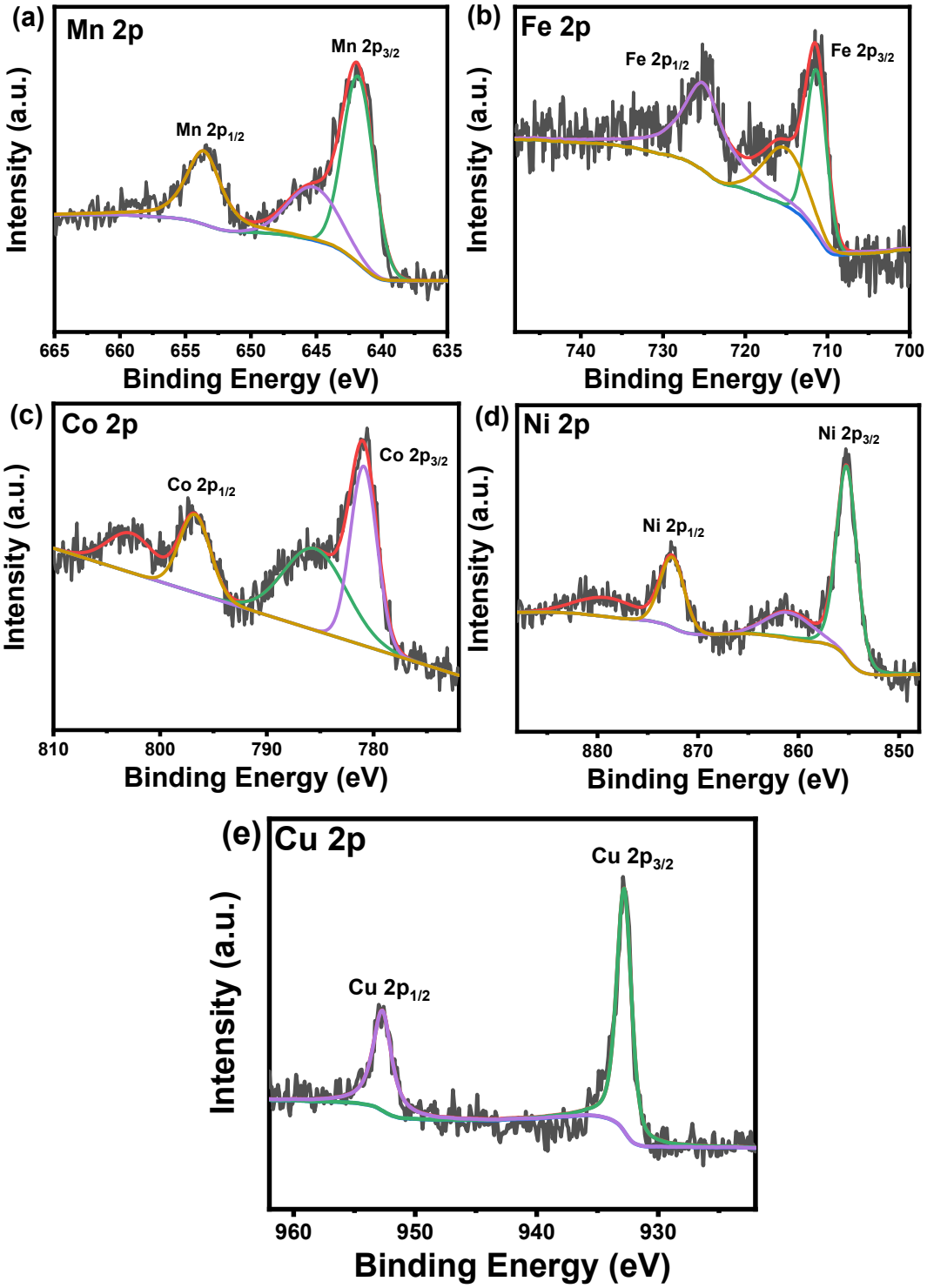

Figure S8. The high-resolution XPS spectra of a) Mn 2p, b) Fe 2p, c) Co 2p, d) Ni 2p and e) Cu 2p.

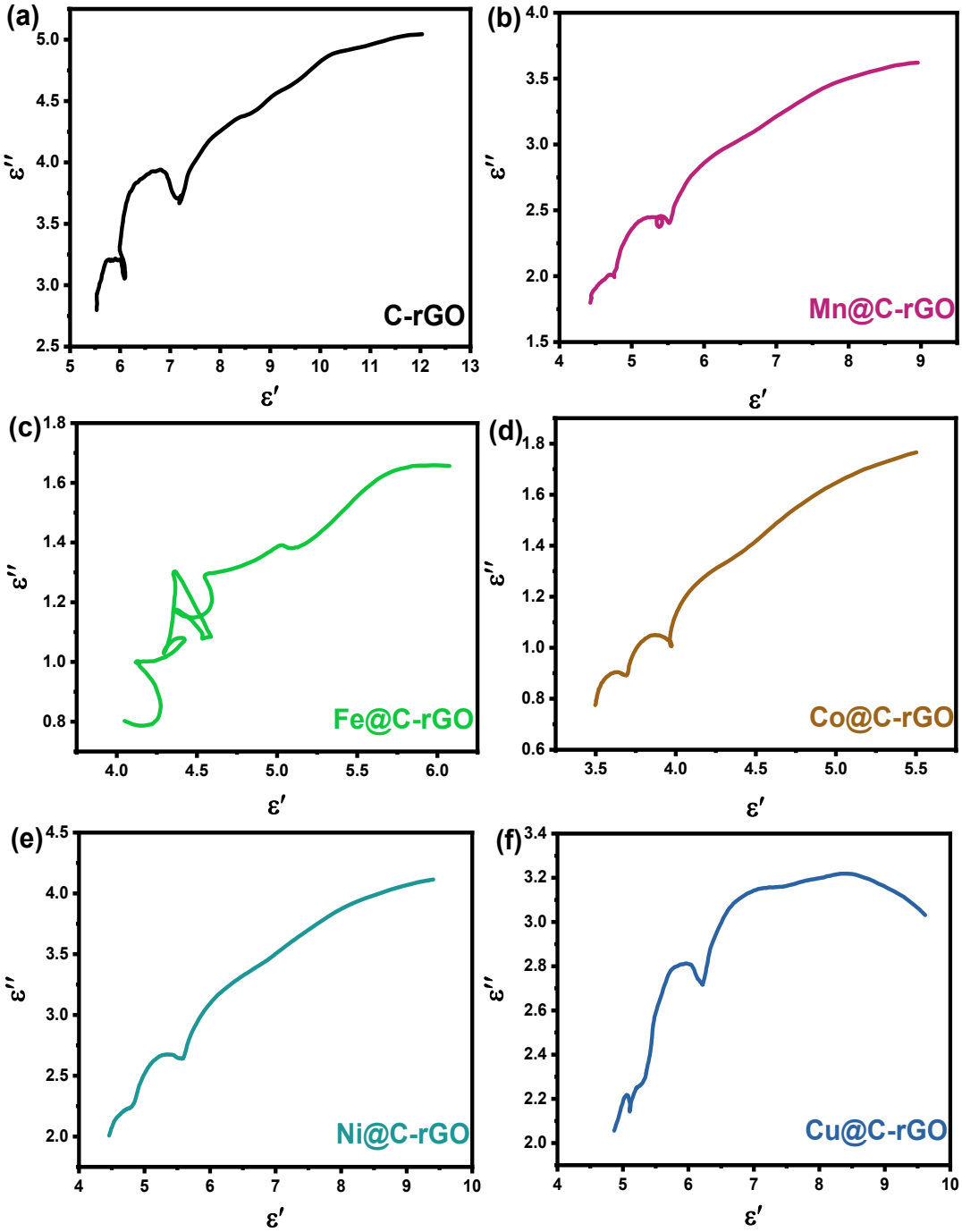

Figure S9. The Cole-Cole curves of a) C-rGO, b) Mn@C-rGO, c) Fe@C-rGO, d) Co@C-rGO, e) Ni@C-rGO and f) Cu@C-rGO.

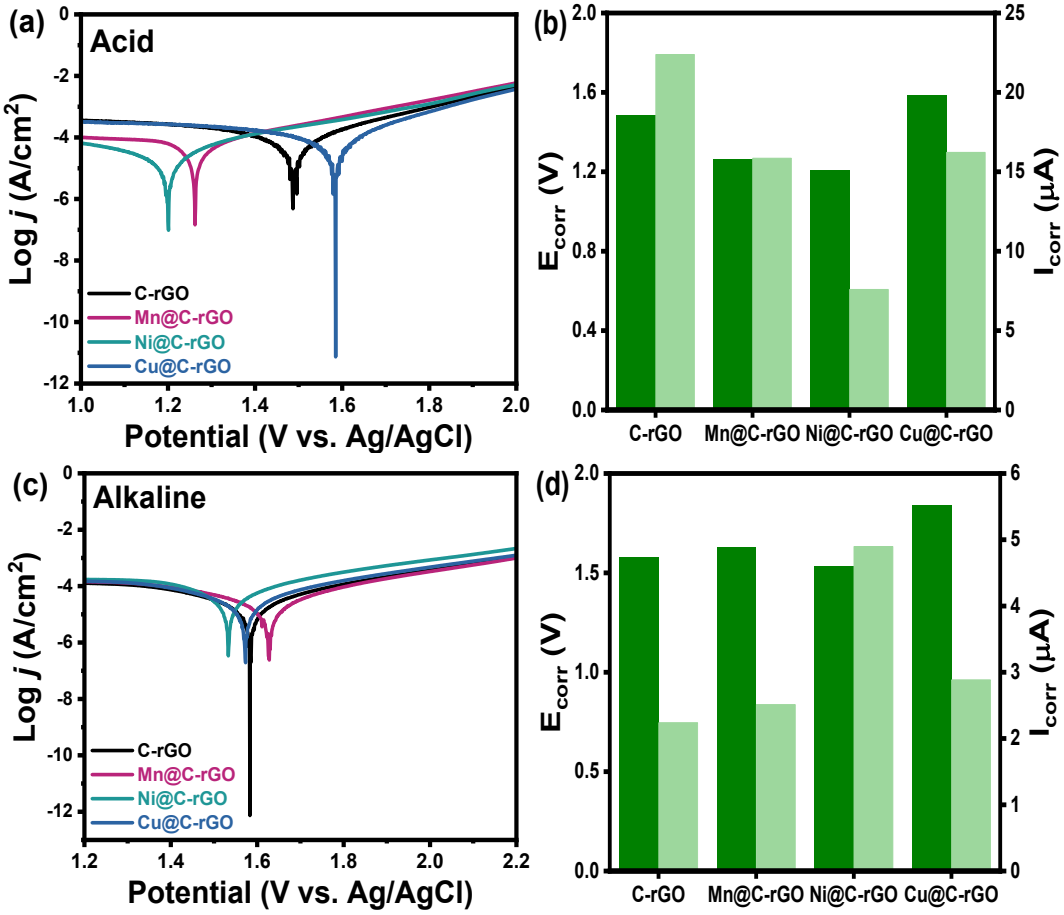

Figure S10. a, c) The Tafel curves and b, d) the I_{corr} and R_p in acidic and alkaline corrosion conditions.

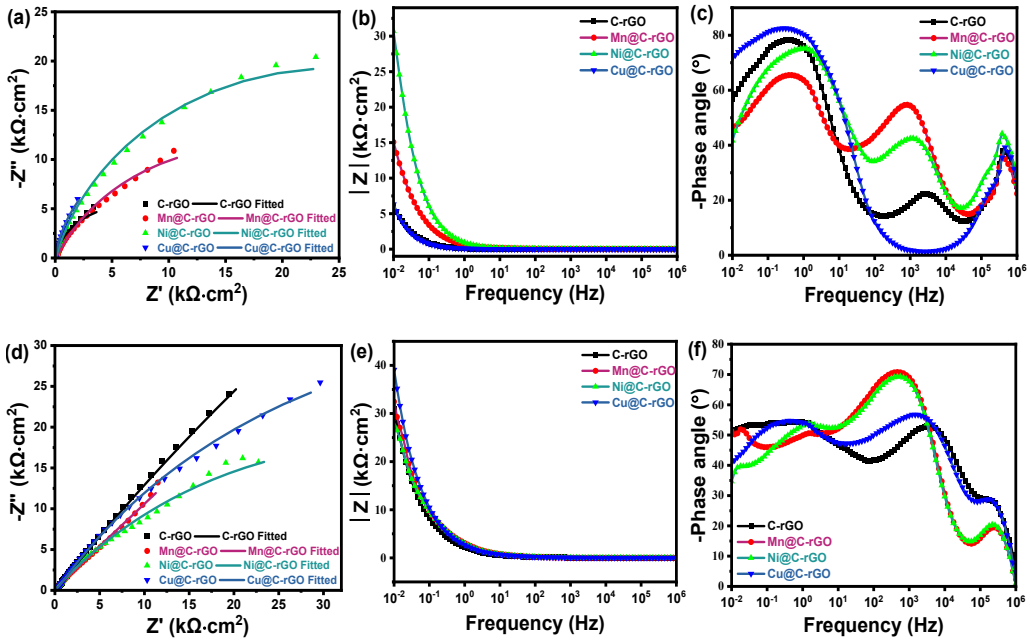

Figure S11. a, d) The Nyquist plots, b, e) Bode plots. c, f) Phase angle plots of in acidic and alkaline solutions.

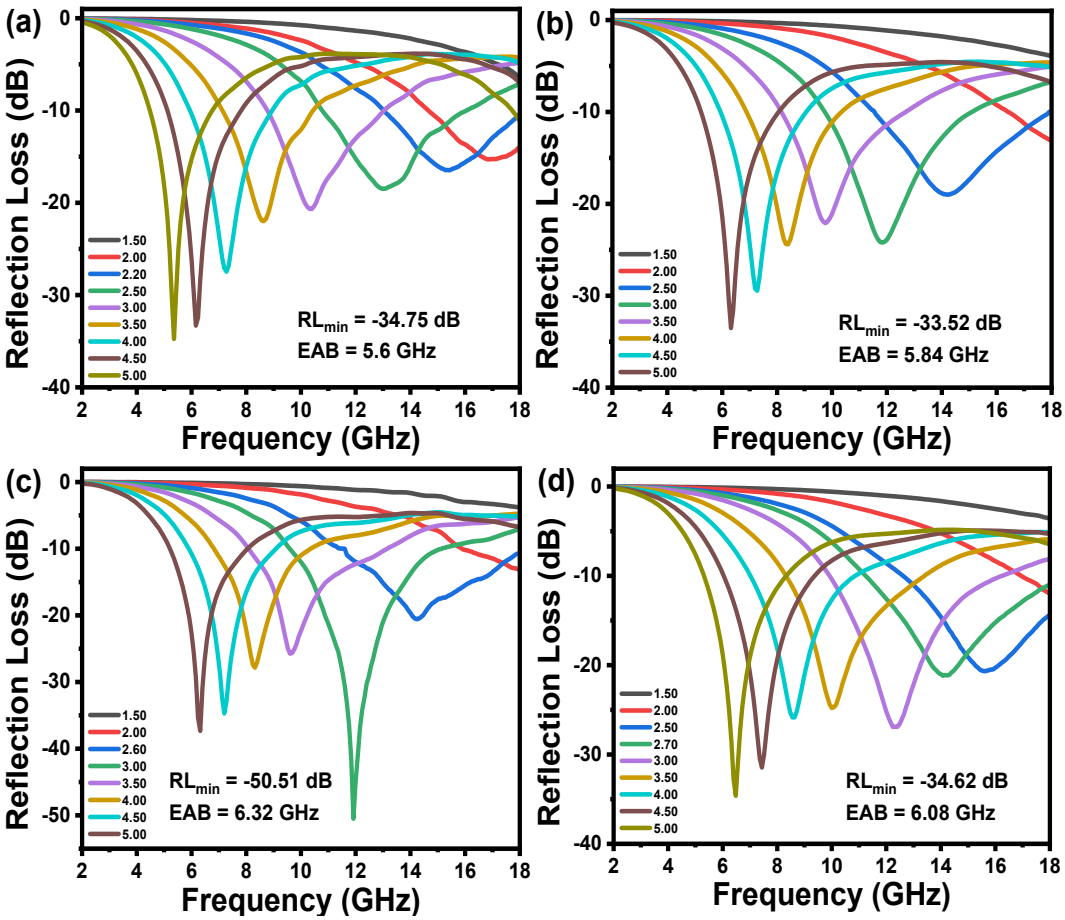

Figure S12. The RL values of a) C-rGO, b) Mn@C-rGO, c) Ni@C-rGO and d) Cu@C-rGO after 7 days of corrosion in 3.5 wt% NaCl solution.

Table S1. Comparison of the RL_{min} and EAB of similar rGO-based.

Sample	RL_{min} (dB)	RL_{min}@Frequency (GHz)	EAB (GHz)	Refs.
FePc/N-rGO	−49.3	5.4	4.2	[S1]
$Mo_2TiC_2T_x$/RGO	−55.1	13.8	5.7	[S2]
NiO@$NiFe_2O_4$/rGO	−55	16.88	6.4	[S3]
RGO/GDY	−58	8.3	4.3	[S4]
$Ti_3C_2T_x$/rGO/NiO	−62.98	7.5	3.1	[S5]
$Ti_3C_2T_x$@rGO@MoS_2	−54.2	16.07	6.04	[S6]
rGO/MXene/TiO_2/Fe_2C	−67.4	8.89	5.68	[S7]
HAg/PANI/GO	−61.14	11.32	4.77	[S8]
AgNWs@NGAs	-79.99	13.92	3.5	[S9]
RGO/CNTs/GDY	−51.8	16.5	5.4	[S10]
$La_{0.8}CoO_3$-rGO	-62.34	12.88	6.08	[S11]
N-doped rGO/g-C_3N_4	−49.59	15.3	4.56	[S12]
MoS_2/PPy/rGO	−53.5	11.76	5.36	[S13]
MXene/rGO	−44.3	7.06	4.84	[S14]
Co@N-RGO	−48.9	11.8	6.0	[S15]
Ni-MOF-rGO	−51.19	17.52	6.32	[S16]
Mn@C-rGO	-53.42	6.88	6.16	This work
Ni@C-rGO	-53.64	7.92	6.64	This work
Cu@C-rGO	-59.28	7.6	6.32	This work

Table S2. The R_{ct} values under acidic, neutral, and alkaline environments.

Sample	R_{ct} under acid (Ω cm^2)	R_{ct} under alkaline (Ω cm^2)	R_{ct} under neutral (Ω cm^2)
C-rGO	1.246×10^4	4.504×10^5	5.841×10^5
Mn@C-rGO	2.850×10^4	3.034×10^5	3.971×10^5
Ni@C-rGO	4.615×10^4	1.191×10^5	2.885×10^5
Cu@C-rGO	3.398×10^4	1.382×10^5	1.421×10^5

References:

[S1] J. Zhang, L. Chen, X. Li, H. Cao, W. Chen, X. Wang, Regulation dipole moments of n-doped graphene coordinated with FePc toward highly efficient microwave absorption performance in c band, Small (2024) 2308459.

[S2] M. Ling, F. Ge, F. Wu, L. Zhang, Q. Zhang, B. Zhang, Effect of crystal transformation on the intrinsic defects and the microwave absorption performance of $Mo_2TiC_2T_x$/RGO microspheres, Small 20 (2024) 2306233.

[S3] L. Yao, Y. Wang, J. Zhao, Y. Zhu, M. Cao, Multifunctional nanocrystalline-assembled porous hierarchical material and device for integrating microwave absorption, electromagnetic interference shielding, and energy storage, Small 19 (2023) 2208101.

[S4] M. Ling, F. Wu, P. Liu, Q. Zhang, B. Zhang, Fabrication of graphdiyne/graphene composite microsphere with wrinkled surface via ultrasonic spray compounding and its microwave absorption properties, Small 19 (2023) 2205925.

[S5] F. Zhang, S. Shang, Y. Li, B. Fan, R. Zhang, B. Zhao, H. Lu, C. Ma, Tunable electromagnetic properties of $Ti_3C_2T_x$/rGO foams decorated with NiO particles, CrystEngComm 24 (2022) 5949-5957.

[S6] Y. Wang, R. Ding, Y. Zhang, B. Liu, Q. Fu, H. Zhao, Y. Wang, Gradient hierarchical hollow heterostructures of $Ti_3C_2T_x$@rGO@MoS_2 for efficient microwave absorption, ACS Appl. Mater. Interfaces 15 (2023) 32803-32813.

[S7] G. Wang, C. Li, D. Estevez, P. Xu, M. Peng, H. Wei, F. Qin, Boosting interfacial polarization through heterointerface engineering in MXene/graphene intercalated-based microspheres for electromagnetic wave absorption, Nano-Micro Lett. 15 (2023) 152.

[S8] W. Fu, W. Yang, C. Qian, Y. Fu, Y. Zhu, One-pot synthesis of Ag/AgCl heterojunction nanoparticles on polyaniline nanocone arrays on graphene oxide for microwave absorption, ACS Appl. Nano Mater. 6 (2023) 3728-3737.

[S9] X. Shu, S. Yan, B. Fang, Y. Song, Z. Zhao, A 3D multifunctional nitrogen-doped RGO-based aerogel with silver nanowires assisted self-supporting networks for enhanced electromagnetic wave absorption, Chem. Eng. J. 451 (2023) 138825.

[S10] M. Ling, P. Liu, F. Wu, B. Zhang, Three-dimensional RGO/CNTs/GDY assembled microsphere: Bridging-induced electron transport enhanced microwave absorbing mechanism, Carbon 214 (2023) 118351.

[S11] L. Chang, Y. Wang, X. Zhang, L. Li, H. Zhai, M. Cao, Toward high performance microwave absorber by implanting $La_{0.8}CoO_3$ nanoparticles on rGO, J. Colloid Interface Sci. 174 (2024) 176-187.

[S12] Q. Su, Y. He, D. Liu, K. Jia, L. Xia, X. Huang, B. Zhong, Facile fabrication of ultra-light N-doped-rGO/g-C_3N_4 for broadband microwave absorption, J. Colloid Interface Sci. 650 (2023) 47-57.

[S13] S. Liu, D. Fang, F. Xing, H. Jin, J. Li, Auricularia-shaped MoS_2 nanosheet arrays coated hierarchical multilayer MoS_2/PPy/rGO composites for efficient microwave absorption, Chem. Eng. J. 479 (2024) 147613.

[S14] X. Li, D. Xu, D. Zhou, S. Pang, C. Du, M. Darwish, T. Zhou, S. Sun, Vertically stacked heterostructures of MXene/rGO films with enhanced gradient impedance for high-performance microwave absorption, Carbon 208 (2023) 374-383.

[S15] L. Wang, R. Mao, M. Huang, H. Jia, Y. Li, X. Li, Y. Cheng, J. Liu, J. Zhang, L. Wu, R. Che, Heterogeneous interface engineering of high-density MOFs-derived Co nanoparticles anchored on N-doped RGO toward wide-frequency electromagnetic wave absorption, Mat. Today Phys. 35 (2023) 101128.

[S16] K. Cao, X. Yang, R. Zhao, W. Xue, Fabrication of an Ultralight Ni-MOF-rGO aerogel with both dielectric and magnetic performances for enhanced microwave absorption: Microspheres with hollow structure grow onto the GO nanosheets, ACS Appl. Mater. Interfaces 15 (2023) 9685-9696.